Cihan University-Erbil Scientific Journal (CUESJ)

Research Article

Optimizing GNSS Data Sampling Rates for Improving Precise Point Positioning Accuracy and Reducing Convergence Time

Shamal F. Ahmed

Department of Civil Engineering, Tishk International University, Kurdistan Region, Iraq

ABSTRACT

Precise point positioning (PPP) is increasingly being used for achieving highly accurate positioning using a single GNSS receiver, particularly in applications such as seismic monitoring and structural health assessments. This study explores the impact of GNSS data sampling rates on PPP accuracy and convergence time by collecting field measurements from five observation points (A, B, C, D, and E) in Erbil, Iraq, using a Leica GS16 instrument. Data were recorded at sample rates of 5, 15, 30, and 60 s for 2 h at each location. Statistical analysis shows that reducing the sampling interval significantly improves the root mean square error (RMSE). For example, at the 5-s sampling rate, the RMSE at point A dropped by 85% from 0.35 m at 15 min to 0.05 m after 120 min. Similarly, at the 60-s sampling rate, the RMSE improved by approximately 80% during the same period. Across all points, the highest accuracy improvements occurred within the first 30–60 min of observation, demonstrating that higher sampling rates help reduce convergence times. However, the benefit diminishes for extended observation durations, suggesting that optimizing the sampling interval is crucial for balancing accuracy and efficiency in PPP applications.

Keywords: Precise point positioning, sample rate, convergence time, accuracy, RTKLIB software

INTRODUCTION

The most popular approach for achieving very precise location with satellite-based is the use of simultaneous carrier-phase measurements with at least two receivers. The gathered raw data should subsequently be post-processed in an office through the appropriate GNSS processing software. In general, this technique requires considerable money, labor, and administrative work. In addition, it does not offer a solution for those requiring coordinates in real-time.[1,2] The Real-Time Kinematic (RTK) approach was first developed to provide an accurate location in real time. In contrast, Network RTK (NRTK) needs several continuously operating reference stations, control center(s), and a communication connection (such as the cellular or internet) to broadcast adjustments to the user. A single-baseline RTK only needs a base station and radio link. The range between the base station and rover is also restricted, generally between 10 and 20 km for single-baseline RTK and between 70 and 100 km for NRTK techniques.[3,4] Nonetheless, these techniques cannot be utilized successfully in certain challenging terrain situations, such as hills surrounded by various terrain types, high mountains, or urban canyons, that prevent or restrict radio access or global system for mobile communication utilization.

Precise point positioning (PPP), whether post-processed or real-time, has recently gained attention. This approach utilizes derived accessible or real-time streaming GNSS satellite products to achieve centimeter to decimeter-level precise positioning globally, all while maintaining a consistent global reference frame. Since 2013, the International GNSS Service (IGS) has offered a global real-time service (RTS) for PPP. In addition, several private companies have developed their own commercial global real-time PPP services as alternatives to IGS-RTS. Furthermore, there are free internet services available, as well as alternatives for commercial, corporate, and academic software for post-processed PPPs.[5-11]

The PPP method, recognized for its numerous advantages, has been extensively applied across various fields, this includes applications in precise positioning, surveying, mapping, monitoring crustal deformation, orbit estimation, agriculture, weather forecasting, construction, and photogrammetry using unmanned aerial vehicles. Data gathering at a very high sample

Corresponding Author:
Shamal F. Ahmed, Department of Civil Engineering, Tishk International University, Kurdistan Region, Iraq.
E-mail: shamal.fatah@tiu.edu.iq

Received: November 4, 2024
Accepted: February 19, 2025
Published: March 30, 2025

DOI: 10.24086/cuesj.v9n1y2025.pp36-40

rate has recently been made feasible because of advancements in GNSS hardware and data processing techniques.[12] Due to these advancements, high-rate GNSS PPP is now widely utilized in seismology and various engineering projects. It plays a crucial role in measuring earthquake displacements, assessing the condition of engineering structures, and calculating the vibrations and displacements of civil engineering assets, including tall buildings, towers, and both long and short-span bridges, as well as viaducts. This technology is particularly important for structures that are susceptible to the impacts of earthquakes, strong winds, or heavy traffic loads.[11-16]

Numerous investigations have looked at how well the typical PPP approach performs, incorporating GNSS observations with a sample rate of 30 s.[6,8,9] An important area of interest for the PPP approach, the influence of the observation sampling rate on PPP performance, specifically the effect of increasing the sample rate on the convergence time, which has not received much attention. The interval of the precise orbit and clock products plays a crucial role in determining positioning accuracy, especially when higher-frequency GNSS observations are utilized, as it can lead to interpolation errors. The recent IGS precise orbit products are expected to have interpolation accuracies better than 0.3 cm.[17] High-rate clock corrections are essential for supporting high-rate PPP applications,[17,18] as random drifts in satellite clocks can lead to significant instability over time.[19] The IGS typically provides precise orbit and clock products at 30-s or 300-s intervals, but high-rate products are not publicly available. To date, there has been limited research on high-rate PPP processing using multi-GNSS combinations. Given the growing integration of high-rate observations with PPP applications, this research aims to explore the impact of the observation sampling rate on PPP performance, particularly with respect to positioning accuracy and convergence time.

METHODOLOGY

PPP Method

PPP combines differential positioning methods with absolute positioning. In addition, it uses a variety of adjustments and it processes data collected from a single GNSS receiver and makes a number of adjustments.[6,20] Because PPP does not rely on connecting observations with simultaneous measurements from reference stations, such as relative baseline positioning does, it provides greater flexibility for operation and is appropriate for regions with limited GNSS network infrastructure.[6,21,22] Even though PPP can produce extremely accurate positioning results, it sometimes needs quite lengthy observation periods to do so. Therefore, the objective of PPP is to reduce its convergence time rather than to enhance the achieved accuracy. If one can eliminate these unidentified ambiguities, one may anticipate noticeably lower convergence durations since the existence of carrier-phase ambiguities heavily influences how long convergence takes. If the possibility of accurately estimating the ambiguities could be made with a high enough success rate, then this is feasible.[4]

For the pseudorange (or code) P^s_{uj} and carrier-phase ϕ^s_{uj} of a user receiver "u" tracking satellite "s" at frequency "j," the observation equations

$$P^s_{uj} = \rho^s_u + \mu j l^s_u + dt_{u.j} - dt^s_j + e^s_{u.j} \quad (1)$$

$$\varnothing^s_{uj} = \rho^s_u + \mu j l^s_u + \delta t_{u.j} - \delta t^s_j + \epsilon^s_{u.j} \quad (2)$$

Where $\rho^s_u = l^s_u + \tau^s_u$ is the sum of the receiver-satellite range l^s_u and the tropospheric delay τ^s_u, and $\mu_j i^s_u$ is the (first-order) ionospheric delay (an advance for phase and delay for code), with i^s_u denoting the ionospheric delay at the first frequency and $\mu_j = (\lambda_j/\lambda_1)^2$ being the ionospheric coefficient, with $\lambda_{j\ being}$ the j-frequency wavelength. The receiver-satellite range, $l^s_u = r^s - r_u$, depends on the unknown, to be determined, user-receiver position r_u at signal reception time $t_R \approx t_E + l^s_u c$ (c = vacuum speed of light) and on the satellite position r^s at the signal emission time t_E. The frequency-dependent user-receiver and satellite clock errors for the code and phase are given as:

$$dt_{u.j} = dt_u + d_{u.j}, dt^s_j = dt^s + d^s_j \quad (3)$$

$$\delta t_{u.j} = dt_u + \delta_{u.j}, \delta t^s_j = dt^s + \delta^s_j \quad (4)$$

Where dt_u and dt^s *are* the common user-receiver and satellite clock offsets and $d_{u,j}$, d^s_j, $\delta_{u,j}$,δ^s_j *are* the frequency-dependent code and phase hardware delays, respectively. The additional unknown parameter $z^s_{u,j}$ in the carrier-phase Eq.(1) is the integer carrier-phase ambiguity. The remaining code and phase errors are denoted by $e^s_{u,j}$ and $\epsilon^s_{u,j}$, respectively. They capture the measurement noise and any other remaining unmodeled effects, such as multipath effects. Henceforth, they will be omitted unless they are truly needed. As a further simplification, the observation equations between the satellites will be used.

Denoting the variate difference between satellites t and s as $(.)^{st} = (.)^t - (.)^s$, the corresponding between-satellite observation equations follow from Eq. (1) as

$$P^{st}_{u.j} = \rho^{st}_u + \mu j l^{st}_u - dt^{st}_j \quad (5)$$

$$\varnothing^{st}_{u.j} = \rho^{st}_u + \mu j l^{st}_u - \delta t^{st}_j + \lambda j z^{st}_{u.j} \quad (6)$$

From now the receiver code and phase clock errors, $dt_{u,j}$ and $\delta t_{u,j}$, have been eliminated. Inspection of this set of observation equations shows that information on the satellite positions and satellite clocks is needed for a *single receiver user* to be able to solve for its unknown parameters. Provision of satellite orbits and clocks dt^{st}_j allows the user data to be corrected, thus resulting in the adapted user equations

$$P^{st}_{u.j} + dt^{st}_j = \rho^{st}_u + \mu j l^{st}_u \quad (7)$$

$$\varnothing^{st}_{u.j} + dt^{st}_j = \rho^{st}_u - \mu j l^{st}_u + \lambda j \alpha^{st}_{u.j} \quad (8)$$

In which $\alpha^{st}_{u.j} = z^{st}_{u.j} + (d^{st}_j - \delta^{st}_j)/\lambda j$ With the satellite positions known and the absence of the unknown dt^{st}_j, δt^{st}_j, this modified system in Eq.(8) has now reached the point where it is possible to find a solution in the event that five or more satellites are tracked on two or more frequencies. The use of accurate orbits and clocks to enable precise single-receiver placement is the fundamental concept behind PPP.[4]

Data Acquisition and Processing

In this study, five measurement points were selected along a 100-m road in Erbil, Iraq, at a latitude of 36.19°E and a

longitude of 44.00°N, on the basis of satellite imagery. Before this selection, a reconnaissance survey was conducted to ensure that all the points were located in open areas without nearby buildings or other obstacles, as illustrated in Figure 1. The selected points were marked on the ground in preparation for instrument setup and subsequent data collection. The observations were commenced by using the PPP method static mode. A Leica GS16 instrument was used to gather the raw data. The row data were observed with a 5 s sample rate and for 2 h at each point. For the post-processing step, the unprocessed RTK Library RTKLIB data were utilized. RTKLIB is an open-source software package created at the University of Tokyo for calculating positions and analyzing GNSS data.[23] Unlike web-based tools, users must manually select the parameters and calculation options. For instance, the software allows the import of precise orbit and clock files. In addition, the user is responsible for selecting an ambiguity resolution method and specifying the desired data output format.

RESULTS AND DISCUSSION

The data presented in the figures (from 2 to 6) provide a detailed statistical comparison of the performance of the GNSS under different sampling rates and time intervals. Beginning with Figures 2-6, the root mean square error (RMSE) values across various sample rates (5, 15, 30, and 60 s) show significant reductions in error as the time intervals increase. For example, in Figure 2, point A shows a RMSE reduction from approximately 0.35 at the 5-s sampling rate after 15 min to 0.05 after 120 min. This represents an approximate 85% improvement in the RMSE over time. Similarly, for the 60-s sampling rate, the RMSE starts at approximately 0.10 at 15 min and decreases to nearly 0.02 after 120 min, yielding an approximately 80% reduction. This pattern is consistent across points B, C, D, and E, with the highest initial errors observed at shorter intervals and faster sample rates, followed by gradual reductions as the sampling duration increases.

For the generalized position Figure 7, the RMSE decreases substantially within the first 30 s, with an overall reduction of approximately 70% from the initial values. This decline is especially pronounced at shorter sampling intervals, indicating that a considerable portion of error correction occurs early on. Over time, the RMSE stabilizes after around 60 s, suggesting a rapid improvement phase followed by convergence to lower error levels. Across all sampling intervals, the accuracy gains are significant, with the largest improvements occurring within the first 5–15 min. These initial gains reflect an approximate 60–80% reduction in RMSE from starting values, underscoring the effectiveness of early sampling for error mitigation.

In the generalized satellite Figure 8, the number of visible satellites remains relatively stable across all time intervals and sampling rates, with fluctuations of <5%. This stability indicates that satellite availability does not significantly impact RMSE improvements; instead, factors, such as sampling rate and observation duration are more influential. For instance, even with a consistent satellite count of around 20, the RMSE shows a marked decline, reinforcing the idea that accuracy improvements are driven primarily by the frequency and duration of observations rather than satellite quantity. This finding highlights the importance of optimizing sampling rates for enhanced positioning accuracy without requiring additional satellite resources.

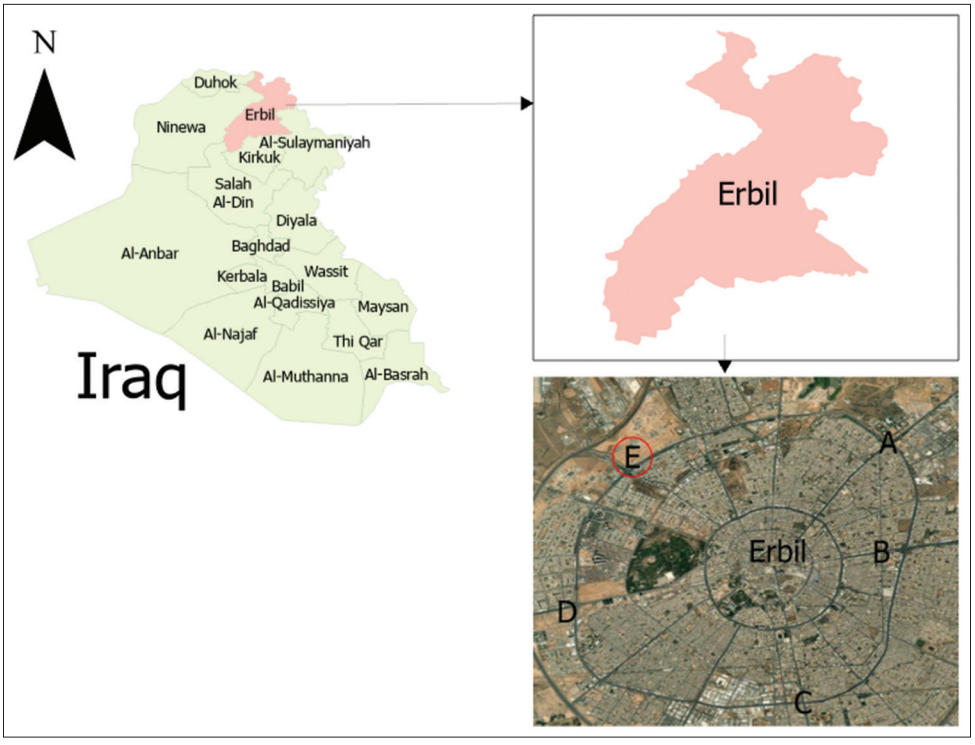

Figure 1: Study area

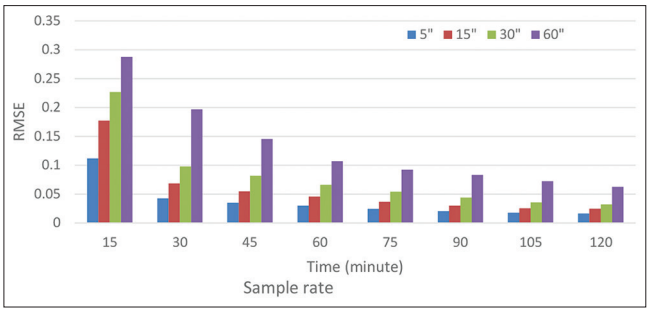

Figure 2: The root mean square error of point A at different times and sampling rates

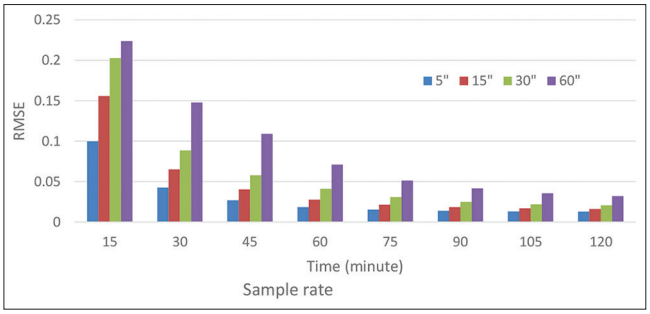

Figure 3: The root mean square error of point B at different times and sampling rates

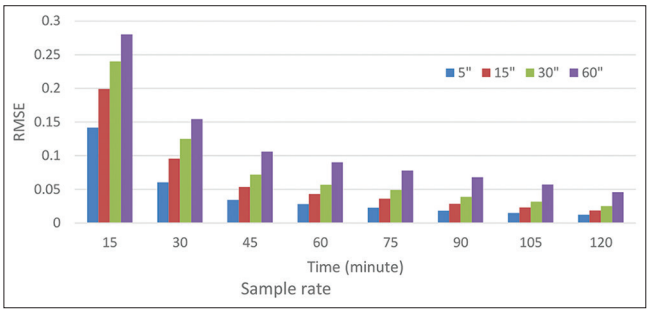

Figure 4: The root mean square error of point C at different times and sampling rates

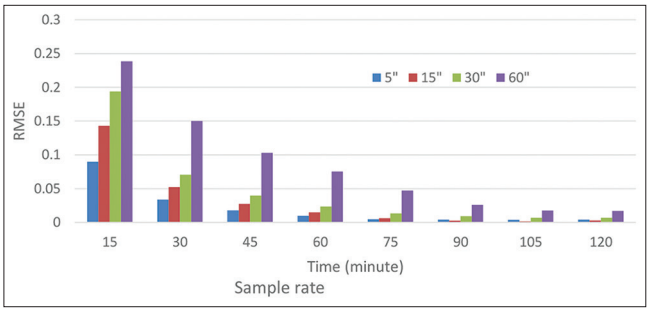

Figure 5: The root mean square error of point D at different times and sampling rates

In conclusion, positioning accuracy improves by approximately 60–85% within the first 30–60 min of observation. Decreasing the sampling rate from 60 s to 5 s can achieve an additional 50% reduction in error within the first 15 min. However, the benefit of higher sampling frequencies

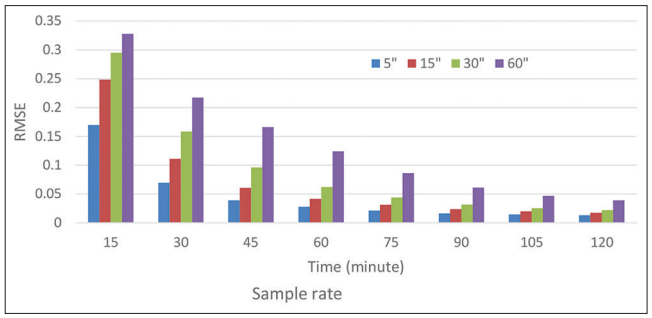

Figure 6: The root mean square error of point E at different times and sampling rates

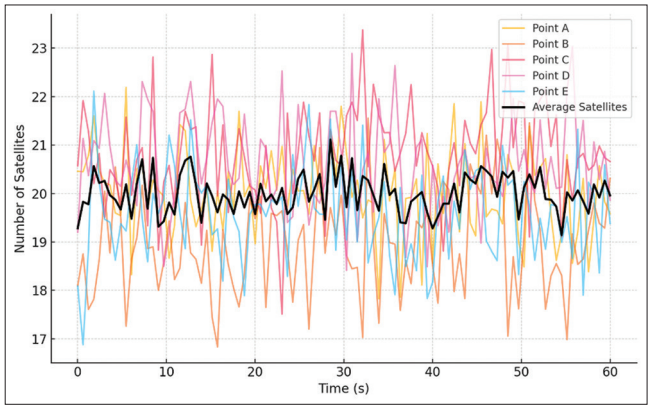

Figure 7: General satellite count over time for all points (A-E)

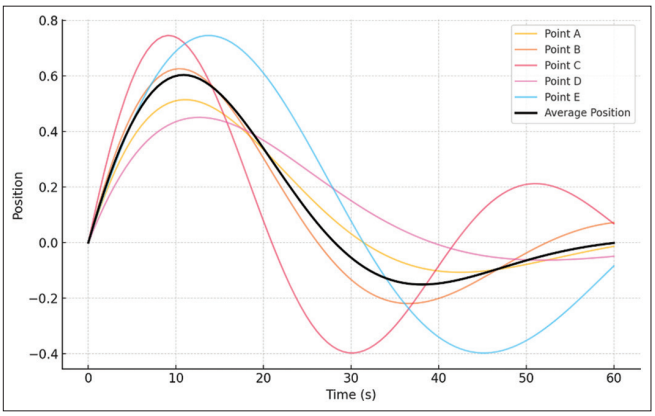

Figure 8: General position over time for all points (A-E)

diminishes over extended observation periods, suggesting that a balanced sampling approach offers the best trade-off between accuracy and efficiency in convergence.

CONCLUSION

This study highlights the significant influence of GNSS data sampling rates on the accuracy and convergence time of PPP. Higher sampling rates, such as 5 s, lead to faster convergence and a significant reduction in RMSE, especially in the first 30–60 min of observation. For instance, the RMSE at point A decreased by 85% when using a 5-s rate, from 0.35 m at 15 min to 0.05 m after 120 min. Similarly, a 60-s sampling rate showed an RMSE reduction of 80% over the same time. This pattern of

rapid early improvement was consistent across all test points, indicating that a higher sampling rate effectively shortens the convergence time and enhances positioning accuracy. However, after the 1st h, the benefits of higher sampling rates diminish, suggesting that while they are useful in short-term observations, their advantage fades over longer periods. The findings also suggest that optimizing the observation duration and sampling rate is crucial for maximizing PPP performance. While high sampling rates yield quick improvements in accuracy, moderate rates, such as 15 or 30 s may suffice for long-term applications as extended observation periods naturally improve accuracy. This balance between sampling rate and duration helps achieve both precision and efficiency in GNSS-based applications. Overall, this study offers practical guidelines for selecting sampling rates based on the specific needs of real-time and long-term PPP applications, making it especially relevant for fields, such as surveying, seismic monitoring, and structural health assessments.

REFERENCES

1. S. F Ahmed. Impact of crowded sky on GNSS positioning. *Polytechnic Journal*, vol. 13, no. 1, pp. 157-163, 2023.
2. S. F. Ahmed. Grid to ground solutions in construction projects. *Cihan University-Erbil Scientific Journal*, vol. 6, no. 2, pp. 161-165, 2022.
3. B. Hofmann-Wellenhof, H. Lichtenegger and J. Collins. *Global Positioning System: Theory and Practice*. Springer Verlag GmbH, Berlin, 2001.
4. P. J. G. Teunissen and O. Montenbruck. *Springer Handbook of Global Navigation Satellite Systems*. 1st ed. Springer International Publishing, New York, 2017.
5. J. F. Zumberge, M. B. Heflin, D. C. Jefferson, M. M. Watkins and F. H. Webb. Precise point positioning for the efficient and robust analysis of GPS data from large networks. *Journal of Geophysical Research*, vol. 102, no. B3, pp. 5005-5017, 1997.
6. J. Kouba and P. Héroux. Precise point positioning using IGS orbit and clock products. *GPS Solutions*, vol. 5, no. 2, pp. 12-28, 2001.
7. M. Ge, J. Douša, X. Li, M. Ramatschi, T. Nischan and J. Wickert. A novel real-time precise positioning service system: Global precise point positioning with regional augmentation. *Journal of Global Positioning Systems*, vol. 11, no. 1, pp. 2-10, 2012.
8. G. Seepersad and S. Bisnath. Challenges in assessing PPP performance. *Journal of Applied Geodesy*, vol. 8, no. 3, pp. 205-222, 2014.
9. S. Choy and K. Harima. Satellite delivery of high-accuracy GNSS precise point positioning service: An overview for Australia. *Journal of Spatial Science*, vol. 64, no. 2, pp. 197-208, 2018.
10. C. Lu, X. Li, J. Cheng, G. Dick, M. Ge, J. Wickert and H. Schuh. Real-time tropospheric delay retrieval from multi-GNSS PPP ambiguity resolution: Validation with final troposphere products and a numerical weather model. *Remote Sensing (Basel)*, vol. 10, no. 3, p. 481, 2018.
11. S. Alcay, S. Ogutcu, I. Kalayci and C. O. Yigit. Displacement monitoring performance of relative positioning and precise point positioning (PPP) methods using simulation apparatus. *Advances in Space Research*, vol. 63, no. 5, pp. 1697-1707, 2019.
12. G. Xu and Y. Xu. *GPS: Theory, Algorithms and Applications*. 3rd ed. Springer Science and Business Media, Germany, 2016.
13. T. Liu, W. Jiang, D. Laurichesse, H. Chen, X. Liu and J. Wang. Assessing GPS/Galileo real-time precise point positioning with ambiguity resolution based on phase biases from CNES. *Advances in Space Research*, vol. 66, no. 4, pp. 810-825, 2020.
14. M. R. Kaloop, C. O. Yigit and J. W. Hu. Analysis of the dynamic behavior of structures using the high-rate GNSS-PPP method combined with a wavelet-neural model: Numerical simulation and experimental tests. *Advances in Space Research*, vol. 61, no. 6, p. 1512, 2018.
15. C. O. Yigit and E. Gurlek. Experimental testing of high-rate GNSS precise point positioning (PPP) method for detecting dynamic vertical displacement response of engineering structures. *Geomatics, Natural Hazards and Risk*, vol. 8, no. 2, pp. 893-904, 2017.
16. I. Kudlacik, J. Kaplon, J. Bosy and G. Lizurek. Seismic phenomena in the light of high-rate gps precise point positioning results. *Acta Geodynamica et Geomaterialia*, vol. 16, no. 1, pp. 99-112, 2019.
17. Y. Shu, Y. Shi, P. Xu, X. Niu, and J. Liu. Error analysis of high-rate GNSS precise point positioning for seismic wave measurement. *Advances in Space Research*, vol. 59, no. 11, pp. 2691-2713, 2017.
18. H. Bock, R. Dach, A. Jäggi and G. Beutler. High-rate GPS clock corrections from CODE: Support of 1 Hz applications. *Journal of Geodesy*, vol. 83, pp. 1083-1094, 2009.
19. M. Wermuth, A. Hauschild, O. Montenbruck, and R. Kahle. TerraSAR-X precise orbit determination with real-time GPS ephemerides. *Advances in Space Research*, vol. 50, no. 5, pp. 549-559, 2012.
20. M. Ge, G. Gendt, M. Rothacher, C. Shi. and J. Liu. Resolution of GPS carrier-phase ambiguities in precise point positioning (PPP) with daily observations. *Journal of Geodesy*, vol. 82, no. 7, pp. 401-401, 2008.
21. G. Wübbena, M. Schmitz. and A. Bagge. PPP-RTK: Precise Point Positioning using state-space representation in RTK networks. In *Proceedings of the 18th International Technical Meeting of the Satellite Division of the Institute of Navigation, ION GNSS 2005*, 2005.
22. Y. Mireault, P. Tétreault, F. Lahaye, P. Héroux and J. Kouba. *Online Precise Point Positioning*. GPS World, pp. 59-64, 2008. Available: https://folk.uio.no/treiken/geo4530/gps0908_innov_v7.pdf [Last accessed on 2024 May 19].
23. F. S. Prol, S., Fabricio, M. Kirkko-Jaakkola, H. Horst, T. Malkamäki, M. Zahidul, H. Bhuiyan, S. Kaasalainen, and I. Fernández-Hernández. Enabling the Galileo high accuracy service with open-source software: Integration of HASlib and RTKLIB, *Gps Solutions*, vol. 28, no. 2, pp. 71, 2024.